The Impact of Low-Latitude Anomalous Forcing on Local and Remote Circulation: Winters 1978/79–1986/87

M. CHELLIAH, J. E. SCHEMM* AND H. M. VAN DEN DOOL

Cooperative Institute for Climate Studies, Department of Meteorology, University of Maryland, College Park, Maryland

(Manuscript received 12 February 1988, in final form 1 July 1988)

ABSTRACT

The impact of anomalous tropical forcing on the anomalous tropical and extratropical circulation is examined by comparing the response of a global steady state linear primitive equation model with observations for nine (1978/79–1986/87) December–January–February (DJF) seasons. Outgoing longwave radiation (OLR) anomalies are used as proxies for tropical latent heat release. Root mean square amplitude and anomaly pattern correlation (APC) are chosen to be the verification tools.

It is shown that with OLR as the only forcing, the linear model produces a fairly realistic level of tropical interannual variability in the wind (both rotational and divergent) and geopotential height fields. The nine DJF's mean skill score, as measured by APC, is highest in the tropics for u, v and Φ between 600 to 900 mb where the mean APC is 0.5–0.6. There is skill in the simulation of both the rotational and divergent components of the circulation. In fact, the APC for the velocity potential at upper levels over the global domain is higher than that of the stream function. In the nine DJF's mean there is a small (APC 0.1–0.3), but significant skill in the Northern Hemisphere high latitudes in u, v and Φ at low levels. Since the explained variance is small, it leads us to conclude that *in the mean*, using our linear model, there is no demonstrable impact of much practical value on the extratropical circulation due to anomalous tropical heating.

On a year-by-year basis, however, the years with exceptionally large OLR perturbations in the tropics are also the years with the best model simulations (high APC) over the globe as a whole and particularly in the tropics. In the ENSO DJF's of 1982/83 and 1986/87, the APC's are considerably above average in all regions including the high latitudes. The explained variance in the u and Φ fields at low levels is about 56% in the tropics and 30% in high latitudes. In these years, the impact of the tropical heating anomalies on the remote high latitude circulation is therefore not only significant but also of practical value. The inclusion of the Hadley circulation in the model's basic state enhances the amplitude of the high latitude response, however, without improving the APC.

The model simulates the Southern Oscillation index (as measured by the Darwin–Tahiti 1000 mb height anomaly) with a correlation up to 0.9, as long as there is heating (cooling) in the lowest 300 mb in the prescribed vertical heating profile.

1. Introduction

Many features of the local and far-field responses to tropical heating anomalies can be simulated with models linearized about a given meridionally and vertically varying zonal flow (e.g., Webster 1972, 1973, 1981; Opsteegh and Van den Dool 1980; Gill 1980; Hoskins and Karoly 1981; Simmons 1982). Because the primary response to a heat source in the tropics is in vertical motion (Holton 1979), extraordinary changes in the tropical latent heat release patterns (such as during the El Niño winter of 1982/83) might perturb, shift, or even reverse major Hadley and Walker cells which would result in global-scale circulation changes (e.g., Quiroz 1983).

The dynamics of the tropical response to tropical heating has been understood reasonably well for some time. However, the nature of the far-field response is less certain. Among others, Opsteegh and Van den Dool (1980), Hoskins and Karoly (1981) and Webster (1981), using simple linear models and idealized heat sources in the tropics, proposed Rossby wave propagation as a mechanism to explain the tropical-middle latitude teleconnections. Horel and Wallace (1981) reported observational evidence of a relation between an El Niño–Southern Oscillation (ENSO) index and the Pacific–North American pattern. Correlations up to 0.5 between tropical indices and middle latitude temperatures and pressures were found by van Loon and Madden (1981).

In this study we intend to show the impact of anomalous tropical forcing on the tropical and extratropical

* Present affiliation: Centel Federal Services Corp., NASA/GSFC, Greenbelt, Maryland.

Corresponding author address: Dr. Muthuvel Chelliah, Climate Analysis Center/NMC/NWS/NOAA, W/NMC 52, WWB, Room 605, Washington, D.C. 20233.

circulation as revealed by a comparison of the response of a steady state linear model with observations for nine (1978/79–1986/87) December–January–February (DJF) seasons. We use outgoing longwave radiation (OLR) anomalies as proxies for tropical latent heat release (Arkin 1984). As tools for comparing the simulated and observed fields we choose the root mean square (rms) amplitude and anomaly pattern correlation (APC). The goal of this study is first to diagnose the effect of observed OLR anomalies on the simultaneous global circulation anomalies and, if successful, ultimately to foreshadow their effects.

Specifically, the motivation for this study comes from earlier work in this area, in particular, by Arkin (1984) and Mureau et al. (1987, referred to as MOW hereafter). Arkin used a linear two-layer, p-coordinate model and MOW used a 15-layer, sigma-coordinate model to compute the response due to anomalous tropical latent heating (derived from OLR). However, Arkin's and MOW's comparisons with observations were restricted to the broad "tropical strip" region of 45°N–45°S (and smaller subdivisions therein) and to the streamfunction field, the computation of which in the limited domain is subject to the imposed boundary conditions. Also, MOW verified their results at only two levels (300 and 700 mb). Mureau et al. (1987) obtained a nine (1974/75 to 1983/84) DJF mean APC of about 0.2 at both levels for the streamfunction, which although statistically significant, is quite low. When the forcing was large (1982/83 ENSO season) they obtained a higher APC.

Our approach in this paper will be similar to that of MOW, but the availability (for verification) of a new global observational dataset enables us to enlarge upon MOW's study in the following ways. Comparison of the simulated fields with observations is extended over the whole globe, in five variables (wind components u and v, geopotential Φ, stream function ψ and velocity potential χ) and at nine pressure levels. A comparison of our model simulations with observations for all variables at all levels over various domains will be offered. More specifically, we will address the following questions:

1) Is there skill in diagnosing the circulation in the higher latitudes of the two hemispheres due to low latitude forcing?
2) Does the skill vary with height? Alternatively, is linear theory equally valid at all levels?
3) Is there any skill in the simulated divergent flow which, after all, is the primary response of the model to the specified tropical heat source.
4) Does the inclusion of the mean meridional circulation (Hadley circulation) in the model enhance the skill in the higher latitudes?

The datasets used in this study are described in section 2 and the model in section 3. The results are presented in section 4. The summary and discussions are given in section 5.

2. Datasets

In this study, we make use of two sets of data. The OLR data are used to derive a proxy of the tropical diabatic heating. The climate diagnostics data base (CDDB) is used both to define the model's basic state and to verify the model's simulations. In the following, a brief description of each of these datasets is given.

a. OLR data

The satellite-measured OLR dataset available since June 1974 on a global 2.5° × 2.5° horizontal grid has been described by Gruber and Krueger (1984). In spite of its shortcomings, it has been shown that OLR is quite useful in monitoring tropical convective activities (Arkin 1979; Liebmann and Hartmann 1982) and in climate variability studies (e.g., Lau and Chan 1983a,b).

We determined the climatological monthly mean values of OLR for December, January, and February for the base period 1978/79–1986/87, so as to coincide with the period over which the CDDB is available. The anomalies in the monthly mean were computed as the departures of an individual monthly mean from the climatological monthly mean. The monthly mean anomalies for the 3 months were then averaged to form the DJF seasonal mean anomaly for each of the 9 yr. This DJF mean anomaly is used to estimate the diabatic heating anomaly in the tropics.

Based on station precipitation data in the central and western Pacific, Arkin (1984) obtained the following linear regression relationship between anomalous rainfall amount and anomalous OLR:

$$R = -0.175 \times \text{OLR} \tag{1}$$

where R represents the seasonal mean rainfall anomaly in mm day^{-1} and the OLR anomaly is expressed in W m^{-2}. This relationship explains about 45% of rainfall anomaly variance. Latent heat release by condensation can then be expressed as

$$Q = (C_p Lg/\Delta p)R \tag{2}$$

where C_p is the specific heat of air at constant pressure, L the latent heat of condensation, g the gravitational acceleration, Q the vertically averaged anomalous heating rate in K day^{-1} and Δp the depth of the layer where precipitation is supposed to occur. The three-dimensional diabatic heating distribution in the tropics was computed using (2) and a predetermined vertical heating profile. Although (1) may not be strictly valid outside the tropical western Pacific, we note that the midtropospheric radiational forcing due to the presence of anomalous cloud cover is proportional to the OLR anomaly. Therefore (1) represents the effect of "cloud radiative forcing" (Ramanathan 1987) in the tropics

and low-middle latitudes as well, and may be meaningful even in areas where the rainfall–OLR anomaly correlation breaks down.

b. CDDB data

The CDDB is part of the Global Data Assimilation System used at the National Meteorological Center (NMC) since October 1978. A description of this dataset can be found in Arkin et al. (1986). Among many other quantities, the CDDB contains monthly mean horizontal and vertical components of the wind, temperature and geopotential heights at nine vertical levels (1000, 850, 700, 500, 300, 250, 200, 100, and 50 mb) on a regular latitude–longitude grid over the globe at 2.5 deg resolution. It should be mentioned that although based on post-initialized analyses, the CDDB winds do contain a divergent component (Rosen and Salstein 1985), a rather important feature since the primary response (of a linear model at least) to tropical forcing is vertical motion. The utility of the CDDB for climate studies has been discussed by Arkin (1982, 1984).

We extracted DJF mean u, v, T and Φ for the 9 years, 1978/79 to 1986/87. Climatologies of these variables are formed based on these 9 years, and the anomalies were obtained at all levels for comparison with model simulations. The climatological DJF zonal mean u, v and T for the basic state of the linear model were calculated from the CDDB dataset. The basic state's vertical velocity ω was calculated from v by vertically integrating the zonal mean continuity equation.

3. Description of model and experiments

We use a global, linear steady state primitive equation model to describe the quasi-stationary circulation of the atmosphere. The three-dimensional structure of wind, mass and temperature anomalies in a time-mean atmosphere can be calculated as a response to prescribed anomalous forcing. The model is fundamentally similar to the two-layer, hemispheric p-coordinate version of Opsteegh and Van den Dool (1980). However, several extensions are made as described below.

The model domain is global, has ten equal-pressure layers in the vertical, and is semispectral in the horizontal plane. The meridional resolution is 3 deg latitude, and ten Fourier waves are used to expand the variables in the longitudinal direction. Centered differences are used in both vertical and meridional directions. A Hadley circulation is included as well as Newtonian damping, Rayleigh friction, and vertical and horizontal ∇^2 diffusion of momentum and temperature. The presence of horizontal diffusion produces the same effect as excessive linear dissipation near the zero wind line in the basic state as used by Simmons (1982), MOW and Nigam et al. (1987). The procedure of Lindzen and Kuo (1969) is employed to solve the resulting system of linear equations efficiently.

For all the experiments reported in this study, the following boundary conditions are used for the model. At the North and South poles, all the variables u, v, ω and Φ are set equal to zero. At the top (0 mb) and bottom (1000 mb), u, v and $\omega = 0$. For Φ, the second derivative (in pressure) is set equal to zero at 100 and 900 mb. Some of these boundary conditions are passive when a mean meridional circulation (MMC) is not included. The model is described in detail by Chelliah (1985) in his attempt to simulate the climatological mean standing waves on the globe during both winter (DJF) and summer (JJA).

The diabatic heating obtained from (2) is a vertically integrated quantity. Hence we must specify the vertical distribution. In this study we prescribe two different vertical profiles, since the vertical distribution of the heating in the real atmosphere is not well known. The first profile is that discussed by Hartmann et al. (1984), which concentrates more of the heating in the upper troposphere. Here we shall refer to a slightly modified version of this profile as the mature cloud cluster (MCC) profile. The second is the classical profile described by Yanai et al. (1973), based on Marshall Islands data, which we shall refer to as the western Pacific (WPAC) profile. Both profiles are shown in Fig. 1.

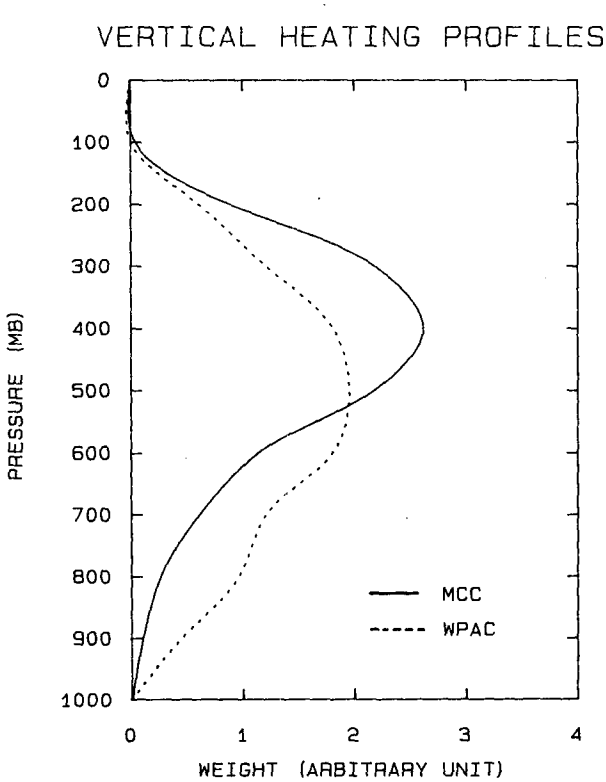

FIG. 1. The two vertical heating profiles used in this study: MCC (standard experiment) and WPAC (sensitivity experiment).

In the remaining sections, frequent reference will be made to the "standard experiment." This is a set of nine model runs for the nine DJF seasons, where the basic state for the model is as described in section 2. In the horizontal plane, the forcing in the 45°S–45°N latitudinal strip is given by (1) and (2) (for a given distribution of OLR), and distributed in the vertical using the MCC profile. Moreover, to insure a smooth meridional transition between the forced and unforced areas, the heating is weighted by $\cos^2(2\varphi)$, where φ is the latitude. The Rayleigh friction coefficient for horizontal momentum has a value of 10^{-6} sec^{-1}, which corresponds to an e-folding time of about 12 days. Rayleigh friction values are slightly larger in the lowest two layers (3.3×10^{-6} sec^{-1} and 6.6×10^{-6} sec^{-1} at 800 and 900 mb, respectively). The Newtonian damping coefficient for temperature at all levels below 200 mb is prescribed as 5.0×10^{-7} sec^{-1}. At the top two layers, the Newtonian damping values are slightly higher (2.75×10^{-6} sec^{-1} and 5.0×10^{-6} sec^{-1} at 200 and 100 mb, respectively). The horizontal diffusion is equivalent to the effect of friction at zonal wavenumber 20.

4. Results

Before we compare the model simulations with the observed circulation anomalies, it should be stressed that it is only in the deep tropics that the latent heating is the most dominant forcing for the atmospheric circulation. Such effects as the transient eddies, mountains and other diabatic effects which force the middle and high latitude circulation are not considered here. It is not our intent to simulate the total observed extratropical anomaly field with tropical diabatic heating as the only forcing.

a. Simulated and observed interannual variability

First, we shall compare the magnitude of the simulated interannual variability (due to tropical latent heating alone) to the observed interannual variability. We have nine DJF global simulations for u, v and Φ at nine levels and their respective observed counterparts. We define the interannual variability for any variable X at any latitude and pressure level as

$$\text{rms}(X) = \left(\frac{1}{M}\sum_i \sum_j (X_{i,j}^2)\right)^{1/2} \qquad (3)$$

where j is the year index (running from 1 to 9) and i is the longitude index (running from 1 to N). Here, N is the number of grid points along a latitude circle and $M = 9N$. Recall that for an anomaly X, $\sum_j X_{i,j} = 0$ by definition. Next, we define an interannual variability ratio for X as

$$\nu(X) = \text{rms}(X_c)/\text{rms}(X_o) \qquad (4)$$

where X_c and X_o are the simulated and observed anomalies (with respect to their 9 DJF mean), respectively, for a particular season. By definition ν cannot be negative, and when it is close to 1 the implication is that the model-produced interannual variability is close to that observed.

Figures 2 and 3 show ν as a function of latitude at 200 and 700 mb for the geopotential and wind [the latter calculated as in (3) and (4) but for $(u_{i,j}^2 + v_{i,j}^2)$] anomalies respectively. The interannual variability generated by the model in the deep tropics is quite comparable to that observed at both levels for both the wind and geopotential fields. This is true at all levels (other levels are not shown). Considering the wide range of values used for dissipation constants in linear models, it is comforting to see that ν is not too far from 1 in the tropics for the reasonable values of the dissipation used in this study. For comparison, the interannual variability of the diabatic heating rate [rms(Q)], as a function of latitude, is shown in Fig. 4. Note that the heating is more confined to the equatorial zone than the response (Figs. 2 and 3). We expected a priori that ν for winds and geopotential would decrease away from the forcing region towards the higher latitudes of either hemisphere. Note, though, in Figs. 2 and 3, that ν is larger in the high latitudes of the Northern Hemisphere than in the Southern Hemisphere. Since the heating is nearly symmetric about the equator (Fig. 4), this asymmetry in ν for the winds and geopotential must be due to the differences in the DJF basic state between the two hemispheres. This is consistent with experiments with idealized heat sources (Hoskins and Karoly 1981) showing that westerlies allow meridional prop-

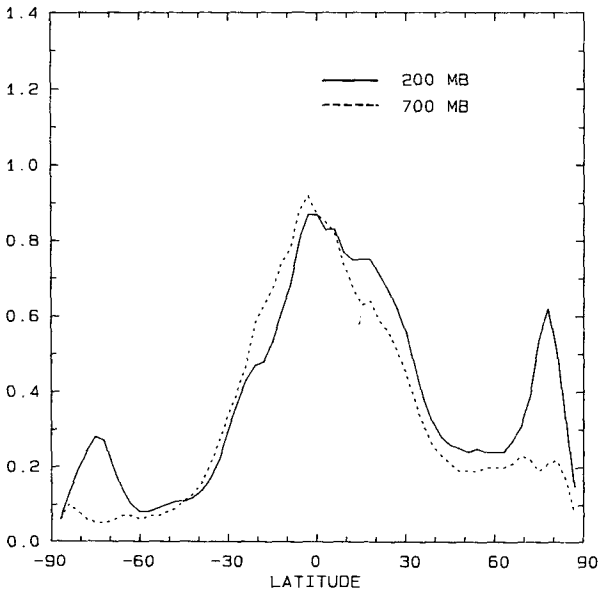

FIG. 2. Interannual variability ratio ν [see (4) for definition] for the geopotential anomaly as a function of latitude at 200 mb (continuous) and 700 mb (dashed).

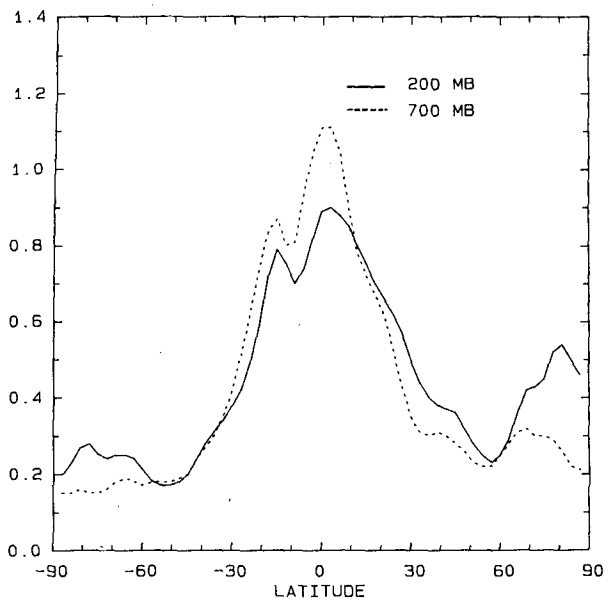

FIG. 3. As in Fig. 2, but for the anomalous wind.

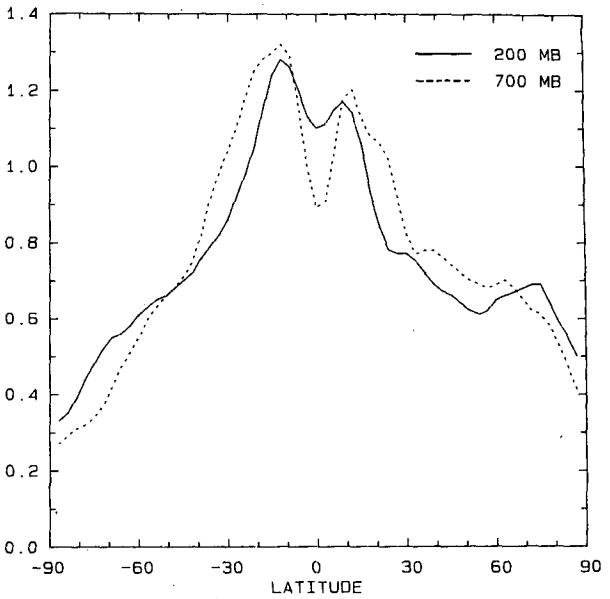

FIG. 5. As in Fig. 2, but for the anomalous divergent wind.

agation. Low ν at high latitudes is also consistent with Kok and Opsteegh (1985), Held and Kang (1987) and Kok et al. (1987), where the importance of the transient eddies (not included here) in forcing the high latitude anomalies was demonstrated.

Recently, Rosen and Salstein (1985) compared the pre- and post-initialized CDDB analyses with each other and with the corresponding analyses from the European Centre for Medium Range Forecasts (ECMWF) for January and July 1983. They concluded that the NMC's adiabatic nonlinear normal mode initialization tended to slightly reduce the strength of the Hadley cell in the tropics. Larger differences were found between the NMC and ECMWF analyses, particularly in the velocity potential field over the western Pacific. With this kind of uncertainty among the "observations," it may not be trivial to get the "correct" interannual variability in the divergent and rotational flow. Figures 5 and 6 are the same as Fig. 3, but now for the divergent and rotational parts of the wind. It is inter-

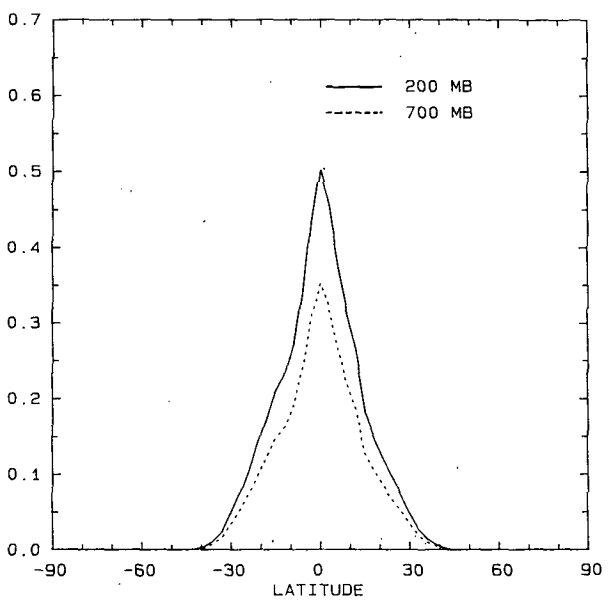

FIG. 4. Interannual variability [measured by rms; see (3)] of the heating rate (model forcing) as a function of latitude at 200 mb (continuous) and 700 mb (dashed).

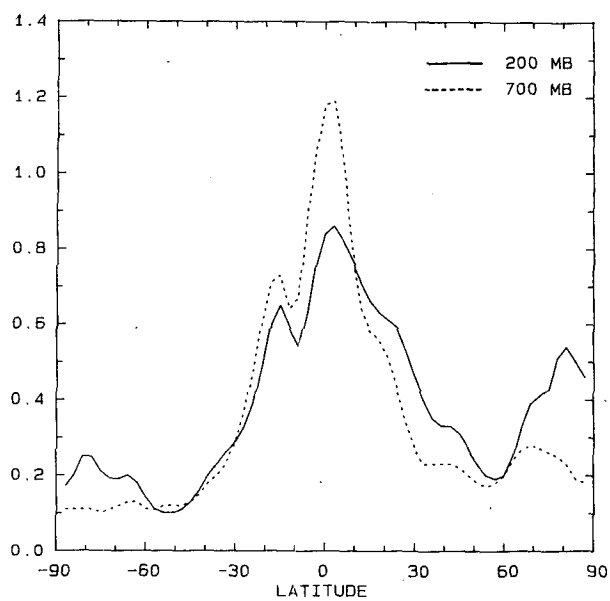

FIG. 6. As in Fig. 2, but for the anomalous rotational wind.

TABLE 1a. Nine DJF mean APC's (in %) for the standard experiment for the anomalous u, v, and Φ as a function of pressure and region. The APC's significant at the 5% level based on a one-sided t-test are denoted by an asterisk. See text for a definition of the various regions.

Level (mb)	u					v					Φ				
	Region					Region					Region				
	GL	SH	NH	BT	NT	GL	SH	NH	BT	NT	GL	SH	NH	BT	NT
100	11	−7	−6	13	16*	5	−8	−3	8*	10*	0	−14	−11	13*	3
200	13*	−2	−3	14*	19*	13*	−6	0	16*	20*	8	−14	−8	19*	20*
300	7	3	3	8	8	10*	−4	1	13*	14*	7	−12	−5	18*	12
400	8	6	12	8	5	13*	−3	4	17*	18*	9	−9	−2	18*	2
500	18*	9	21*	19*	27*	17*	−1	8	20*	29*	14*	−3	4	21*	32*
600	27*	8	29*	29*	42*	18*	1	12	21*	35*	16*	1	10	20*	48*
700	35*	8	30*	37*	50*	19*	2	13*	21*	34*	17*	5	13	19*	51*
800	36*	6	30*	39*	49*	17*	0	12*	20*	35*	14*	4	13*	14	45*
900	31*	4	28*	33*	41*	14*	0	12*	16*	25*	11*	3	14*	11	33*

esting to see that ν is reasonably close to 1 in the tropics for both the rotational and irrotational flow.

b. *Anomaly pattern correlations*

In this section we examine how well the simulated anomalies compare to the observed anomalies for all nine DJF seasons as a function of height for five variables u, v, Φ, ψ and χ. This will be done by computing the (area weighted) anomaly pattern correlation (APC) coefficient (Van den Dool 1983). It should be mentioned that among the five variables, only u, v and Φ are solutions of the model, while ψ and χ are subsequently calculated from u and v on the globe.

It is clear from Figs. 2, 3 and 4 that even though the forcing is confined to the equatorial zone, its influence is far-reaching. To examine the degree of similarity of the simulated and observed fields both in the tropics and in the remote high latitudes, we computed the APC (over all longitudes) in the following five domains:

GL global (87°S–87°N)
SH Southern Hemisphere (S.H.) high latitudes (87°S–45°S)
NH Northern Hemisphere (N.H.) high latitudes (87°N–45°N)
BT broad tropical strip (45°S–45°N)
NT narrow tropical strip (21°S–21°N)

It should be noted that the APC over the globe (GL) and the broad tropics (BT) are dominated by the response in the NT region. This is because most of the high amplitude response is in the narrow tropics (see Figs. 2, 3, 4). We first present and discuss the nine DJF mean APC[1] for all variables at all levels and in all five regions. Then we present time series of the APC for a few variables at selected levels. Third, we present, in more detail, the APC for the major 1982/83 and more recent 1986/87 ENSO events. In the following discussions we will use the expression "higher (lower) skill" synonymously with "higher (lower) APC between computed and observed fields."

The nine DJF mean APC for the anomalous u, v, and Φ at nine pressure levels for the five regions is shown in Table 1a. A close examination of Table 1a leads to the following inferences:

1) The nine DJF's mean APC for u, v and Φ at all nine levels is positive over the entire globe (GL) and in the 45°S–45°N (BT) and 21°S–21°N (NT) regions.

2) In these three regions, the APC for all the three variables is higher (about twice) in the lower troposphere (600–900 mb) than in the upper troposphere (100–400 mb).

3) There is statistically significant (see Appendix) skill in the high latitude simulations of u, v and Φ in the Northern Hemisphere, but only at low tropospheric levels.

4) The u, v and Φ fields are simulated with higher skill in the higher latitudes of the Northern Hemisphere (NH) than the Southern Hemisphere (SH). This result is consistent with the asymmetry in the interannual variability ratio ν discussed in section 4a and in Figs. 2 and 3.

5) In the 9 yr mean, there is practically no skill for u, v and Φ at the upper levels of the higher latitudes of either hemisphere.

Table 1b is the same as Table 1a, but for ψ and χ. It should be pointed out that since ψ and χ by themselves have no well-defined local meaning (Hendon 1986; Sardeshmukh and Hoskins 1987), trying to interpret the APC's for ψ and χ over any region smaller than the globe could be misleading. We nevertheless give the APC's in subglobal regions for comparison with MOW. (Their values are given in parentheses.) Our mean APC for ψ at both 300 and 700 mb over the tropics (NT and BT) is not too different from

[1] We calculate the nine DJF's mean APC by two different methods. In the first method, we calculate the mean APC by computing the APC for each of the nine DJF's separately and then average over the nine cases. In the second method, we compute a single APC for the nine DJF's by computing the correlation between the juxtaposed nine DJF maps of the respective variables. In general, the mean APC computed by the second method is slightly and uniformly higher. All results presented here are for the first method.

TABLE 1b. As in Table 1a but for streamfunction ψ and velocity potential χ. Values in parentheses are from MOW.

Level (mb)	ψ Region GL	SH	NH	BT	NT	χ Region GL	SH	NH	BT	NT
100	14	−9	−8	17*	23*	34*	40*	23	34*	36*
200	16*	−6	−4	18*	22*	48*	54*	15	49*	55*
300	11	−15	−1	13 (20)	12 (16)	36*	45*	5	37*	42*
400	9	−13	0	12	8	15	2	6	17	20
500	17*	13	1	20*	31*	1	−3	−10	2	4
600	23*	21*	4	26*	47*	17	18	−1	17	21
700	29*	26*	4	32* (22)	57* (40)	31*	39*	7	31*	35*
800	25*	23*	1	28*	56*	35*	35*	9	35*	39*
900	15*	21*	−1	16*	47*	28*	26*	−1	29*	35*

MOW, even though our results indicate better skill at low levels. From Table 1b, the following can be said about the skill in ψ and χ:

(a) On the global domain ψ verifies nearly the same as u and v in Table 1a, with most of the skill at lower levels.

(b) The velocity potential turns out to be simulated generally as good as, or even better than, the streamfunction. One noteworthy difference is that χ is simulated better than ψ at upper levels.

(c) The low APC in u, v, Φ, ψ and χ at the midtropospheric levels in the NT strip and elsewhere is due to the weak amplitude associated with the baroclinic nature of the response. At these midtropospheric levels, verification of ω would, by our APC measure, have shown maximum skill.

Further implications of these results are postponed to the discussion in section 5.

c. *Time series*

We choose 200 and 700 mb as representative levels and u as a representative variable for a discussion of the time series of APC. This is not to say that for each individual DJF, 200 and 700 mb are the levels with the highest APC (see section 4d). Although we used the same vertical profile (MCC) for all DJF seasons, it could very well be that this profile is more appropriate in certain DJF's than in others. Next we show in Figs. 7 and 8 the time series of the APC for u at 700 and 200 mb, respectively. The top panel is for the global and the two tropical regions, and the middle panel is for the two high latitude regions. Also shown for comparison in these figures (bottom panel) is the time series of the strength of the forcing as measured by the spatial rms[2] (over 21°S–21°N) of the diabatic heating rate.

It is clear that at 700 mb (Fig. 7), the 21°S–21°N region (NT) has the highest correlation in all DJF, followed by the 45°S–45°N region (BT), which, in turn, is followed closely by the global region (GL). It is encouraging to note that the correlation is positive in all years. Comparing the three curves in the top panel in Fig. 7 with the time series of the rms heating rate in the bottom panel, we find that, in general, the stronger the forcing, the higher the APC. This result is in agreement with MOW. A similar relationship does not hold between the tropical forcing and the high latitude APC's (middle panel), especially for the Southern Hemisphere, where the amplitude of the model response is, in gen-

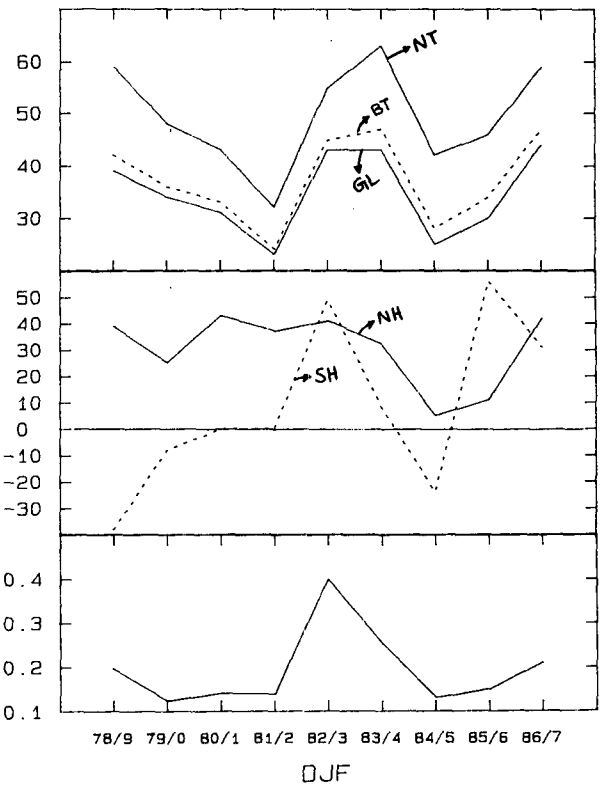

FIG. 7. Time series of APC (%) at 700 mb for u in regions NT, BT, GL (top panel) and NH, SH (middle panel). The rms of heating rate in °K day^{-1} over NT (bottom panel). See text for a definition of the regions.

[2] As in Eq. (3) but with no summation over the index j.

TABLE 2. The APC (in %) for the anomalous u, v and Φ as a function of pressure and region for the DJF seasons of 1982/83 (top) and 1986/87 (bottom). The APC's significant at the 5% level based on a one-sided t-test are denoted with an asterisk. See text for a definition of the regions. See Appendix for significance text.

Level (mb)	u					v					Φ				
	Region					Region					Region				
	GL	SH	NH	BT	NT	GL	SH	NH	BT	NT	GL	SH	NH	BT	NT
							1982/83								
100	52*	28	40	53*	59*	17	17	57*	11	25*	26	11	52	16	20
200	55*	30	24	56*	64*	35*	27	48*	35*	50*	43*	23	45	45*	60*
300	41*	41*	18	43*	53*	33*	25	42*	34*	47*	38*	20	37	41*	54*
400	36*	47*	23	38*	50*	32*	24	43*	31*	39*	34	19	34	35	36
500	12	56*	28	11	4	29*	21	44*	27*	20	34	21	36	35	26
600	21	52*	36	22	27	31*	15	43*	31*	31*	33	13	33	35	56*
700	43*	49*	41*	45*	55*	35*	5	40*	36*	37*	36*	7	32	40	75*
800	60*	39	38	62*	71*	34*	−3	34	37*	46*	30	−6	23	34	78*
900	65*	37	35	68*	75*	22*	−11	34	23*	37*	26	−11	26	29	62
							1986/87								
100	35	14	−13	39	42	12	−30	4	14	27*	16	−7	13	29	41
200	26	25	0	28	30	19	−31	8	21	31*	22	−19	19	33	49
300	23	31	13	26	30	13	−28	12	15	25	21	−24	24	29	34
400	21	37*	26	21	18	10	−27	15	9	20	24	−24	31	29	7
500	27*	40*	36	27	31	14	−23	19	13	34*	29	−15	38	32	44*
600	37*	35	43*	39*	51*	19*	−20	21	21*	46*	31	−7	41	36	66*
700	44*	31	42*	47*	59*	21*	−15	19	23*	43*	33	0	41*	39	73*
800	34*	27	40	36	44	22*	−12	17	26*	50*	33	1	38*	40	74*
900	21	18	29	21	23	21*	−10	12	24*	37*	30	7	37	37	66

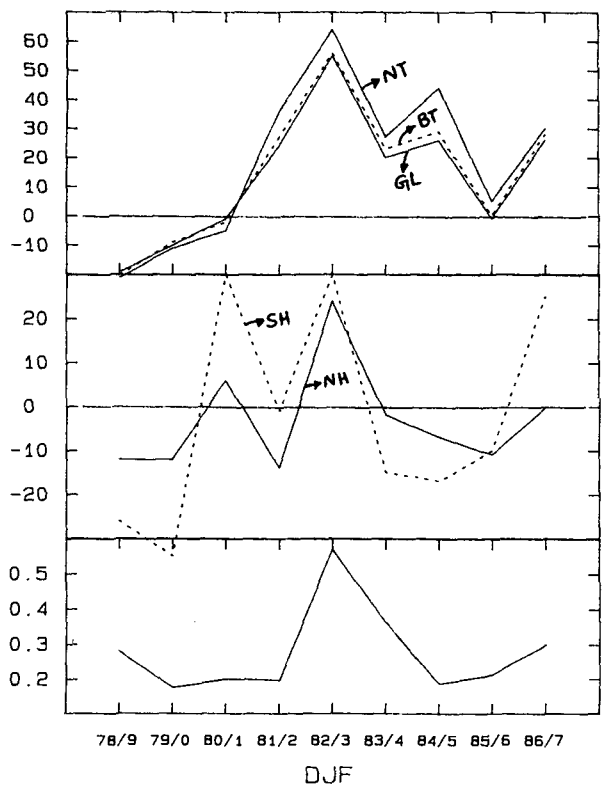

FIG. 8. As in Fig. 7, but for 200 mb.

eral, weak (Figs. 2 and 3). Note, however, that the APC in the high latitudes of the Northern Hemisphere is positive in all years and greater than 0.35 in five out of nine DJF seasons.[3] These five DJF seasons include the major 1982/83 ENSO and the recent 1986/87 ENSO. Incidentally, these two DJF seasons have moderately high APC in the high latitudes of the Southern Hemisphere as well.

At 200 mb (Fig. 8), unlike 700 mb, the relationship between the amplitude of the forcing and the APC over the three regions is less clear. In the high latitudes (middle panel), the APC's are generally low except for the 2 ENSO years and 1980/81.

d. The ENSO DJFs

We next examine in detail the results for the two ENSO DJF seasons of 1982/83 and 1986/87. Table 2 displays the APC for u, v and Φ at nine levels and five regions for the 1982/83 DJF (top) and 1986/87 DJF (bottom). First note that the APCs are generally high

[3] Compared to the other eight DJF's, the forcing for the 1978/79 DJF season is based on fewer OLR measurements, and hence may not be completely representative of the "true" convective activity in the tropics. There are no OLR measurements at all for December 1978. During January and February 1979 there are many days and regions where the OLR observations are either missing or based on interpolated values.

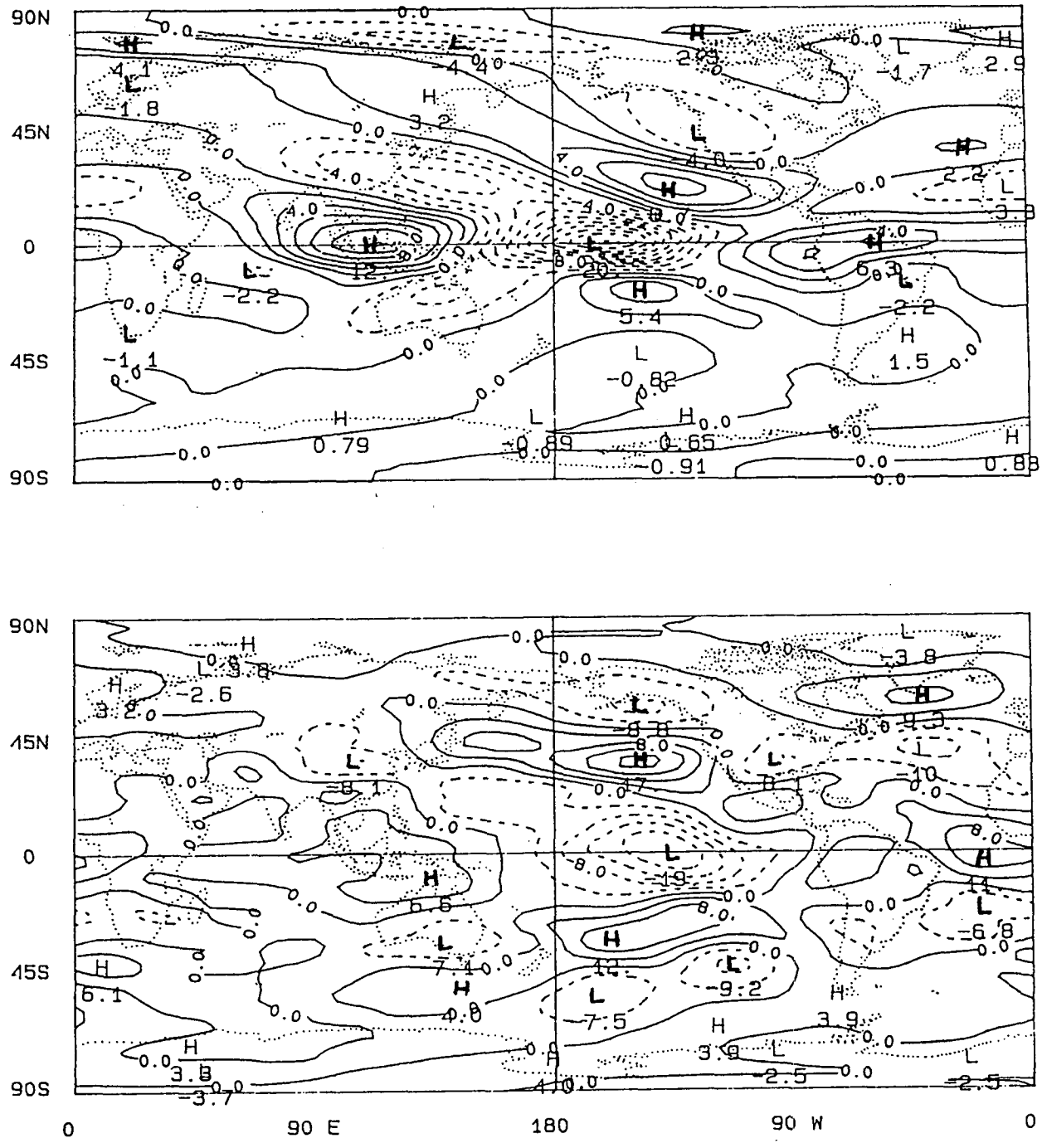

FIG. 9. Simulated (top) and observed (bottom) anomalous u in m s^{-1} for 1982/83 DJF season at 200 mb. Contour interval 2 m s^{-1} top panel and 4 m s^{-1} bottom panel. Negative contours are dashed. The APC for the five regions are NT 64%, BT 56%, NH 24%, SH 30%, and GL 55%.

and mostly positive (except for v and Φ over SH in 1986/87). In particular, unlike the nine DJF mean case (Table 1), there is appreciable skill at many levels in the high latitudes. Consequently, the APC over the whole globe for most variables at several levels is high. For example, the global APC for u at 200 and 800 mb is 0.55 and 0.60, respectively, for the 1982/83 DJF season. In the NT strip, the APC's are near 0.75 at lower levels for u and Φ in both ENSO events.

Shown in Figs. 9 and 10 are the simulated anomalous u at 200 and 800 mb, respectively, for the 1982/83 DJF season. Also shown are the corresponding observed anomalies. The amplitude of the model simulations is quite comparable to the observed amplitude

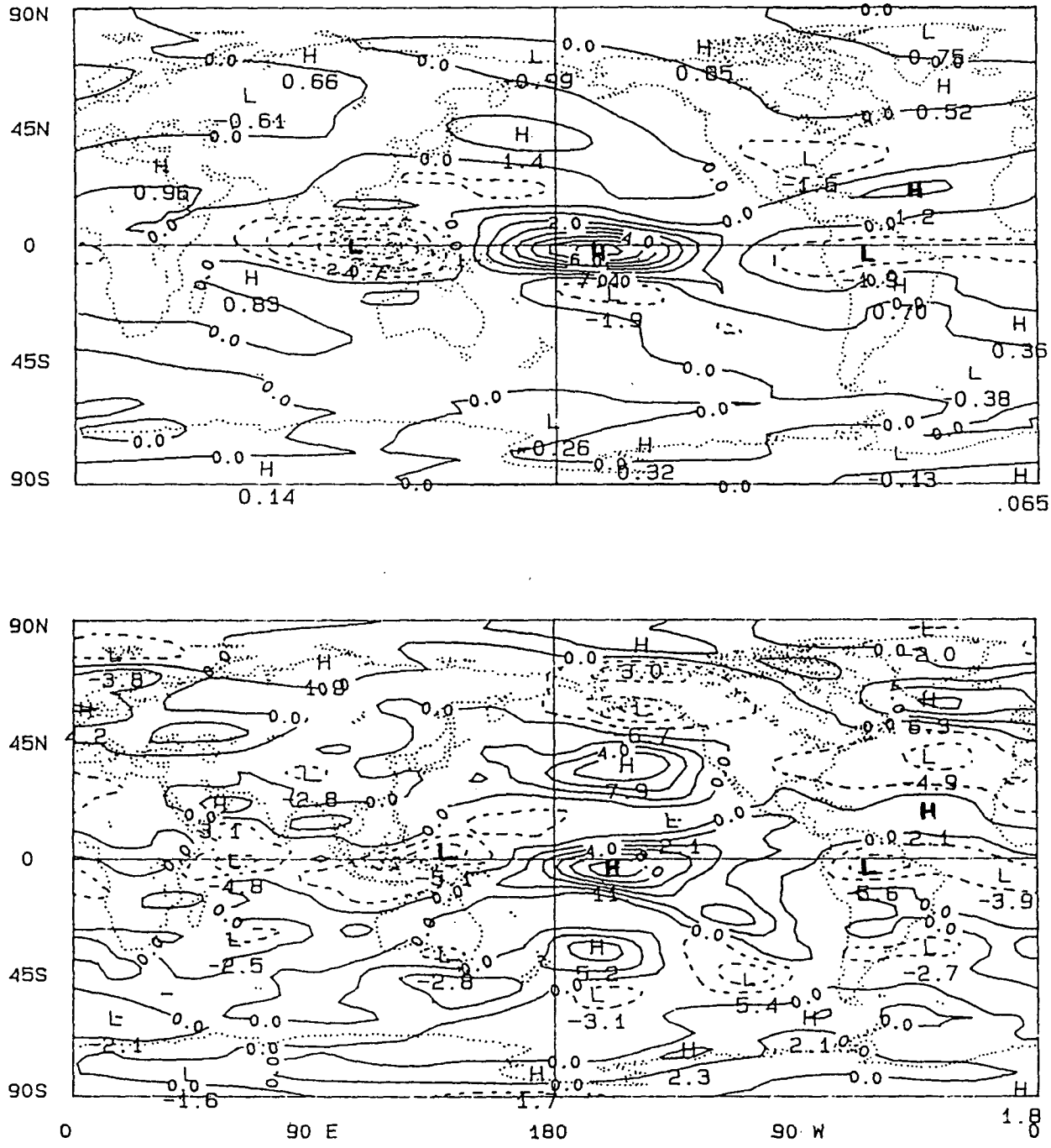

FIG. 10. As in Fig. 9, but for 800 mb and contour interval 1 m s^{-1} top panel and 2 m s^{-1} bottom panel. The APC for the five regions are NT 71%, BT 62%, NH 38%, SH 39%, and GL 60%.

in the deep tropics. Note that the model captures the acceleration of the subtropical zonal wind at 200 mb to the north and south of the heat source. The equatorial westerlies at 800 mb are simulated very well. However, the simulated easterlies at 200 mb are phase-shifted (about 30–40 deg) to the west.

Even though 1986/87 DJF is considered a minor ENSO (Kousky 1987), the skill of the simulation is almost as good as in 1982/83 (Table 2). The results for the ENSO years are probably among the best illustrations of the degree of validity, and hence the applicability, of linear theory. It should, however, be emphasized again that there is skill in all years (see Figs. 7 and 8), including the less studied anti-ENSO years of which DJF 1983/84 is a good example.

The 1982/83 El Niño has recently received a lot of

attention in various general circulation modeling (GCM) studies. (GCM simulations are usually made by prescribing the observed SST anomalies, as opposed to specifying OLR anomalies.) Hence, it is of interest to compare our results to those obtained with a GCM. For example, Shukla and Fennessy (1988) obtained an APC of 0.55 between their simulated and observed geopotential anomalies during 1982/83 at 300 mb over the region 20°S–20°N. This is almost equal to the APC of 0.54 obtained in this study (see Table 2).

e. Sensitivity experiments

1) VERTICAL HEATING PROFILE

All results presented so far are for the standard experiment, where the MCC profile is used to distribute the heating in the vertical direction. In Table 3, results with the WPAC profile are presented to illustrate the effect of changes in the vertical heating distribution. A comparison of Tables 1 and 3 indicates that, overall, the APC's are higher with the MCC profile than with the WPAC profile thereby giving support to the proposed mature cloud cluster profile by Hartmann et al. (1984). Mureau et al. (1987) reached a similar conclusion about the two vertical profiles. However, the anomalous geopotential height in the lowest three levels of the model in the tropics is better simulated (as measured by APC) with the WPAC profile than with the MCC profile. For example, Fig. 11 shows the Southern Oscillation index (SOI) as computed from the model 1000 mb geopotential height difference between Darwin and Tahiti (Darwin–Tahiti) for nine DJF seasons. Also shown is the corresponding observed sea level pressure difference. The correlation between the model and observed SOI is 0.91 (while with the MCC profile (standard experiment) the correlation is only 0.31). Further experimentation showed that it is the difference in heating in the lowest 300 mb (WPAC profile vs MCC profile) that produced the large-scale sea level pressure seesaw in the linear model.

To our knowledge, this result is new. None of the previous studies using linear models (with the possible exception of Webster 1973) reported a high correlation between the simulated and observed anomalous surface heights (pressures) associated with the Southern Oscillation. Webster (1973) correlated his model-simulated geopotential height "anomaly" (departure of seasonal average from the annual mean) at 750 mb for the four seasons at Djakarta and Bombay with all grid points over the globe and obtained a correlation map resembling the Southern Oscillation. While Webster's calculation is based on intraannual climatology, our calculations are more strictly comparable to Walker's (1923) station-pair correlations based on interannual anomalies. Lau (1985) examined the response of a low order GCM by prescribing the observed interannual sea surface temperature (SST) fluctuations in the tropical Pacific Ocean during the period 1962–76. He reported that the simulated Darwin–Tahiti sea level pressure difference (SO index) is correlated very well with the prescribed SST anomaly in the central Pacific. Also, Fennessy and Shukla (1988) simulated a realistic Southern Oscillation in a GCM in response to SST anomalies observed in 1982/83.

TABLE 3. As in Table 1 but with WPAC vertical heating profile.

Level (mb)	u Region GL	SH	NH	BT	NT	v Region GL	SH	NH	BT	NT	Φ Region GL	SH	NH	BT	NT
100	7	−15	−18	10	17*	1	−18	−12	7	12*	−9	−18	−17	1	6
200	9	−10	−14	11	18*	8	−13	−7	11*	17*	−1	−16	−15	9	19*
300	2	−5	−9	3	6	5	−12	−5	8*	10*	−2	−17	−15	7	11
400	−3	0	−3	−3	−6	4	−12	−5	7*	6	−3	−17	−16	6	−2
500	−4	1	3	−5	−10	4	−12	−3	8*	4	−2	−16	−15	6	−11
600	12*	3	11	13*	29*	13*	−11	0	17*	33*	3	−15	−10	9	41*
700	26*	5	16*	29*	45*	15*	−10	4	19*	33*	8	−13	−4	13	51*
800	29*	8	21*	31*	44*	17*	−9	8	20*	36*	12	−11	1	16	53*
900	25*	8	22*	27*	36*	18*	−7	12*	21*	31*	15*	−9	7	19*	50*
	ψ					χ									
100	13	−9	−19	17	25*	41*	48*	35*	41*	42*					
200	14	−14	−18	17	23*	51*	55*	19	52*	57*					
300	6	−22	−17	10	12	40*	47*	8	41*	45*					
400	0	−25	−14	2	−1	29*	29*	15	30*	32*					
500	1	−9	−11	4	−10	26*	33*	37*	27*	23*					
600	19*	11	−5	24*	45*	32*	42*	14	33*	35*					
700	28*	23*	−3	32*	58*	36*	47*	13	37*	40*					
800	25*	21*	−7	28*	58*	29*	32*	7	30*	33*					
900	16*	20*	−8	18*	51*	29*	31*	−3	30*	35*					

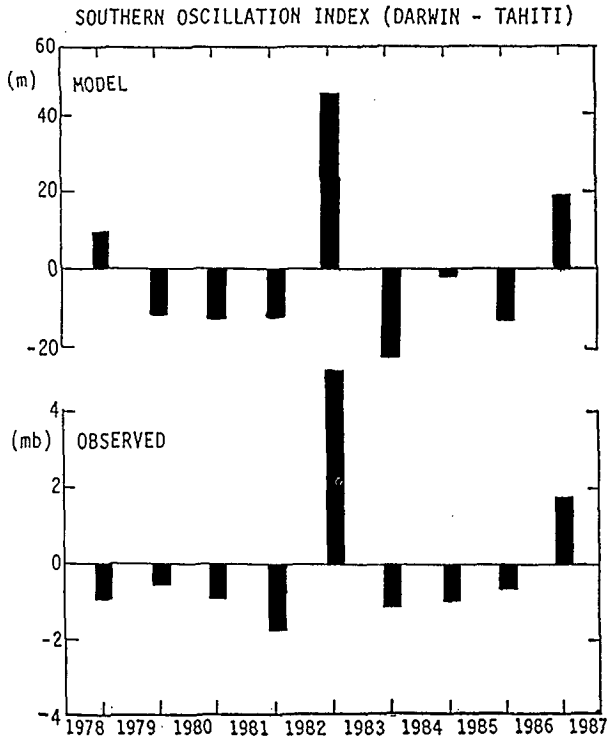

FIG. 11. A Southern Oscillation index (Darwin–Tahiti) computed from the model's 1000 mb height anomaly (top) and observed sea level pressure anomaly (bottom) for nine DJF seasons. The correlation between the two is 0.91.

2) INFLUENCE OF HADLEY CELLS IN THE MODEL'S BASIC STATE

Opsteegh (1982), using a global two-layer linear model, performed a simple experiment to examine the influence of the Hadley cells (MMC) on the model solution. Using a January climatology as the model's basic state, he showed that for an idealized heat source placed in the midlatitudes of one hemisphere, the inclusion of the MMC resulted in considerable energy transport through the easterlies to the other hemisphere. Schneider and Watterson (1984) arrived at similar conclusions about the influence of the MMC.

Because our "standard experiment" already included the MMC (section 3), in the next sensitivity experiment we therefore removed the MMC from the model's basic state. In our experiment most of the heating is confined to the deep tropics in the region of zonal easterlies. Hence, one would expect that the amplitude of the extratropical anomalies would be less in the absence of the Hadley cell. Also, since the Rossby wave propagation affects mostly the rotational part of the flow, the rotational winds should be more affected than the divergent winds. To demonstrate this, we define an interannual variability ratio μ for a variable X as

$$\mu(X) = \text{rms}(X_c^{\text{No MMC}})/\text{rms}(X_c^{\text{MMC}}) \qquad (5)$$

where X_c^{MMC} and $X_c^{\text{No MMC}}$ are the simulated anomalies with and without the MMC. Note that the definition of μ in (5) is very similar to the definition of ν in (4). The ratio μ as a function of latitude is shown in Fig. 12 for the rotational (Fig. 12a) and divergent (Fig. 12b) components of the wind at 200 and 700 mb. Note that for the rotational wind, μ is about 1 in the tropics and subtropics and falls off to lower values towards the poles, implying that without the MMC the interannual variability in higher latitudes is reduced. On the other hand, for the divergent wind, μ is very close to 1 at all

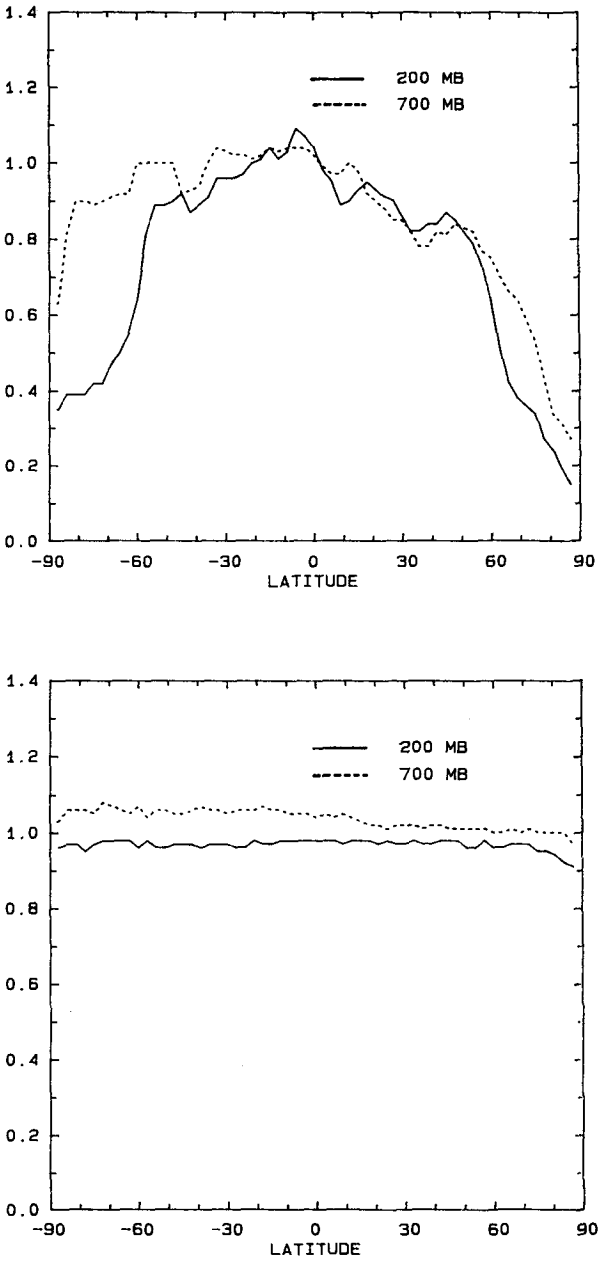

FIG. 12. Interannual variability ratio μ [see (5) for definition] as a function of latitude at 200 mb (continuous) and 700 mb (dashed) for rotational wind (top) and divergent wind (bottom).

latitudes at both levels implying negligible impact of the MMC. Taking out the MMC reduces the amplitude of the high latitude rotational response in both hemispheres, but the impact is larger in the Northern Hemisphere. A probable explanation for this is that the climatological DJF mean Hadley circulation is northward at upper levels (Opsteegh 1982).

We calculated the nine DJF season's mean APC for the no-MMC experiment for u, v, Φ, ψ and χ at all nine levels and for the five different regions. The results (not shown) were compared with Table 1 (standard experiment). We find that the APC in the tropics (BT and NT) are essentially the same in both experiments. In higher latitudes (SH and NH), where we expected some differences, the correlations are not noticeably different either. Apparently, the increased amplitude (with MMC) does not translate into increased resemblance (in phase) with the observed anomalies in higher latitudes.

5. Summary and discussion

In this paper we have examined the possible impact of anomalous tropical forcing on the contemporaneous tropical and extratropical circulation anomalies during the DJF season. This was done by comparing the response of a steady state linear model with observations for nine DJF seasons (1978/79–1986/87). Observed OLR anomalies for these nine seasons were used as proxies for tropical latent heat release, which is the linear model's forcing. The comparison was made at nine pressure levels over the whole globe for three variables (u, v and Φ) in terms of rms amplitude and anomaly pattern correlation (APC). We also considered results for the streamfunction and velocity potential. The main conclusions of this study are as follows:

1) With just OLR forcing, our linear model produced a fairly realistic level of interannual variability in the tropical wind (both rotational and divergent parts) and geopotential height anomalies.

2) The nine DJF's mean APC for u, v and Φ is positive at all levels (100–900 mb) over the 21°S–21°N, and 45°S–45°N regions and over the globe. The highest skill (i.e., highest APC) is found in the tropics (mean APC of about 0.5–0.6).

3) In the 9 yr mean, there is a small (APC 0.1–0.3) but significant skill in the Northern Hemisphere high latitudes in u, v and Φ at low levels. Because the explained variance is small, we conclude that, in the mean, there is no demonstrable impact of much practical value of the anomalous tropical heating on the extratropical circulation.

4) The years with strong OLR anomalies are (overall) also the years with the best simulations (high APC).

5) In the ENSO DJF's of 1982/83 and 1986/87, the APC's are considerably above average in all regions including the high latitudes. The explained variance in the anomalous u and Φ fields at low levels is about 56% in the tropics and about 30% in the high latitudes. In ENSO years the extratropical response is not only significant but also interesting from a practical point of view.

6) The inclusion of the Hadley circulation (MMC) in the basic state enhances the amplitude of the response in the high latitudes but does not improve the APC.

7) Overall, better simulations are obtained with the MCC vertical heating profile than with the WPAC profile. However, the Southern Oscillation index as measured by the Darwin–Tahiti sea level pressure is better simulated with the WPAC profile, which allows for modest heat release in the lowest 300 mb.

8) In the global domain, for the 9 yr mean, there is statistically significant skill in the simulation of velocity potential. In fact APC's for χ are higher than those for ψ at upper levels.

Specifying tropical heating in a linear model is almost identical to specifying vertical motion, at least at the midtropospheric levels of the deep tropics. Thus, the model's tropical vertical motion should be correctly simulated to the extent that the atmospheric heating is known. Although the observed vertical motion may not be perfectly known, we note the significant correlation between observed and calculated velocity potential both at lower and upper levels. Therefore, there is skill in the model's *primary* response.

When verifying the wind, which is mostly rotational even near the equator (Sardeshmukh and Hoskins 1985), we are, in fact, checking the *secondary* responses of the model to the heating. The results indicate that our linear model exhibits a reasonable skill in simulating the streamfunction, but mainly at low levels.

The relatively low skill (in u, v and Φ) at the upper levels (as compared to lower levels) in the tropics turns out to be due to the well-known "phase problem" with linear models (Hendon 1986). Using a simple viscous linear model, Gill (1980) demonstrated why the pair of anticyclones (the main upper level response) would develop to the west of upper tropospheric divergence. Kok et al. (1987) address the phase shift found in linear models' response in middle and higher latitudes as well. Our model produces a reasonable looking upper level tropical response, but phase shifted to the west by about 30–40 deg of longitude (see Fig. 9). Experiments with different dissipation parameters did not alleviate the phase error. The vorticity budget studies of Sardeshmukh and Held (1984) and Sardeshmukh and Hoskins (1985) suggest that in the tropical upper troposphere nonlinearities could very well be important.

There is little doubt that the mechanism that creates the *tropical* circulation anomalies is the year-to-year change in the Walker circulation. This is anticipated given the results of many model studies using idealized heat sources (Webster 1981 in particular) and the results of model studies in which realistic heating was prescribed (Webster 1973; Arkin 1982; MOW). Given that the linear model's extratropical response in some

years resembles observed anomalies, we conclude that at least one of the mechanisms of the *tropical–extratropical teleconnection* is contained in a linear model. We note two mechanisms: (1) The acceleration of the *subtropical* jets is due to changes in the thermally direct Hadley overturning at a given longitude. This mechanism is the same as the one operating through the Walker cell. (2) The anomalies in the *middle and high latitudes* are at least partially a consequence of the Rossby wave propagation of energy from the tropics into the high latitudes, aided and modified perhaps by instability of the zonal mean basic state (Branstator 1985).

Recently, Hendon (1986) made a representation of an equatorially trapped Kelvin wave in terms of the velocity potential and streamfunction. He pointed out that both ψ and χ gave the appearance of significant velocity perturbations in the individual components away from the equator, despite the known trapping within 10 degrees of the equator. In fact, for these equatorially trapped waves, away from the equator $u_\psi = -u_\chi$ and $v_\psi = -v_\chi$. Thus a successful simulation of a tropical phenomenon may give the false impression of positive APC in ψ and χ over remote domains. Therefore, it could be misleading to limit the verification in remote areas to either the streamfunction or the velocity potential alone, as was done in Arkin (1984) and MOW.

Previous studies (Opsteegh 1982; Schneider and Watterson 1984) have proposed that the inclusion of the MMC in the model's basic state facilitates Rossby wave propagation through easterly layers. We indeed found that the MMC enhances the amplitude of the mid- and high latitude response, but does not increase the APC's. Compared to other potential improvements that can be made in the basic state (such as longitude dependence), the inclusion of MMC appears to be only a minor issue.

The linear model performs reasonably well in simulating the global three-dimensional anomalous atmospheric circulation, especially when and where the anomalous tropical forcing is large. Because we do not prescribe a complete three-dimensional forcing, however, correlation with the observed anomalies remains rather low especially in higher latitudes. Rainfall is not very well known over much of the globe, and using OLR as a proxy has validity only in the deep tropics. In principle, one can use a GCM and extract all the quantities needed to calculate the forcing of the time mean flow in a GCM. Nigam et al. (1986) and Kok et al. (1987) have indeed shown that under these circumstances, a linear simulation resembles the GCM results rather well even in high latitudes. It seems, therefore, that one of the main problems in modeling *observed* anomalies is the lack of knowledge about the complete three-dimensional forcing anomalies.

Acknowledgments. This work was supported by the Cooperative Institute for Climate Studies under NOAA Grant NA84-AA-H-00026. We thank Drs. Brant Liebmann, Åke Johansson, the two reviewers, and Dr. R. Rosen (editor) for their thoughtful comments. The data used in this study were kindly provided to us by John Janowiak of the Climate Analysis Center.

APPENDIX

Significance of Anomaly Pattern Correlation

The statistical significance of the anomaly pattern correlations has been tested in the following way. At a given level (and, e.g., for u) we have computed APC (u_c^i, u_o^j), where the subscripts c and o refer to the calculated model and observed values, and the year indices $j \neq i$ range from $j = 1, 9$ and $i = 1, 9$. Therefore, in total, there are 72 $(81 - 9)$ APC's between nonmatching years which have a near zero mean. We have used the standard deviation (sd) of this distribution to test whether the APC (u_c^j, u_o^j) for the matching years is positive and different from zero. The null hypothesis is that u_c^j and u_o^j are not positively correlated. We reject the null hypothesis if APC $(u_c^j, u_o^j) > 1.645$ sd based on a one sided t-test at the 5% level.

The significance of the 9 yr mean APC is tested by checking whether the 9 yr mean APC is greater than $1.645\ \text{sd}/\sqrt{9}$, i.e., we assume the nine cases to be independent. In Tables 1, 2 and 3, APC values denoted by an asterisk are significant according to the test described above. Our testing procedure is almost identical to that in Kok and Opsteegh (1985).

REFERENCES

Arkin, P. A., 1979: The relationship between fractional coverage of high cloud and rainfall accumulations during GATE over the *B*-scale array. *Mon. Wea. Rev.*, **107**, 1382–1387.

——, 1982: The relationship between interannual variability in the 200 mb tropical wind field and the Southern Oscillation. *Mon. Wea. Rev.*, **110**, 1393–1404.

——, 1984: An examination of the Southern Oscillation in the upper tropospheric tropical and subtropical wind field. Ph.D. dissertation, University of Maryland, 240 pp.

——, V. E. Kousky, J. E. Janowiak and E. A. O'Lenic, 1986: Atlas of the tropical and subtropical circulation derived from National Meteorological Center operational analysis. NOAA Atlas No. 7. [Available from Climate Analysis Center (NMC), National Weather Service, Washington, D.C. 20233]

Branstator, G., 1985: Analysis of general circulation model Sea-surface temperature anomaly simulations using a linear model. Part I: Forced solutions. *J. Atmos. Sci.*, **42**, 2225–2241.

Chelliah, M., 1985: Summer and winter global stationary eddy patterns due to mountains and diabatic heating. Ph.D. dissertation, University of Maryland, 156 pp.

Gill, A. E., 1980: Some simple solutions for heat induced tropical circulations. *Quart. J. Roy. Meteor. Soc.*, **106**, 447–462.

Gruber, A., and A. F. Krueger, 1984: The status of NOAA outgoing longwave radiation data set. *Bull. Amer. Meteor. Soc.*, **65**, 958–962.

Hartmann, D. L., H. H. Hendon and R. A. Houze, 1984: Some implications of the mesoscale circulations in tropical cloud clusters for large scale dynamics and climate. *J. Atmos. Sci.*, **41**, 113–121.

Held, I. M., and I.-S. Kang, 1987: Barotropic models of the extratropical response to El Nino. *J. Atmos. Sci.*, **44**, 3576–3586.

Hendon, H. H., 1986a: The time-mean flow and variability in a nonlinear model of the atmosphere with tropical diabatic forcing. *J. Atmos. Sci.*, **43,** 72–88.

——, 1986b: Stream function and velocity potential representation of equatorially trapped waves. *J. Atmos. Sci.*, **43,** 3038–3042.

Holton, J. R., 1979: An Introduction to Dynamic Meteorology. Academic Press, 391 pp.

Horel, J. D., and M. J. Wallace, 1981: Planetary scale atmospheric phenomena associated with the interannual variability of sea surface temperature in the equatorial Pacific. *Mon. Wea. Rev.*, **109,** 813–829.

Hoskins, B., and D. Karoly, 1981: The steady linear response of the atmosphere to thermal and orographic forcing. *J. Atmos. Sci.*, **38,** 1179–1196.

Kok, C. J., and J. D. Opsteegh, 1985: Possible causes of anomalies in seasonal mean circulation patterns during the 1982–83 El Niño event. *J. Atmos. Sci.*, **42,** 677–694.

——, J. D. Opsteegh and H. M. van den Dool, 1987: Linear models: Useful tools to analyze GCM results. *Mon. Wea. Rev.*, **115,** 1996–2008.

Kousky, V. E., 1987: The global climate for December 1986–February 1987: El Niño returns to the tropical Pacific. *Mon. Wea. Rev.*, **115,** 2822–2838.

Lau, N. G., 1985: Modelling the seasonal dependence of the atmospheric response to observed El Niños in 1962–76. *Mon. Wea. Rev.*, **113,** 1970–1996.

Lau, K. M., and P. H. Chan, 1983a: Short-term climate variability and atmospheric teleconnections from satellite observed outgoing longwave radiation. Part I: Simultaneous relationships. *J. Atmos. Sci.*, **40,** 2735–2750.

——, and ——, 1983b: Short-term climate variability and atmospheric teleconnections from satellite observed outgoing longwave radiation. Part II: Lagged Correlations. *J. Atmos. Sci.*, **40,** 2751–2767.

Lindzen, R. S., and H. L. Kuo, 1969: A reliable method for the numerical integration of a large class of ordinary and partial differential equations. *Mon. Wea. Rev.*, **97,** 732–734.

Liebmann, B., and D. L. Hartmann, 1982: Interannual variations of outgoing IR associated with tropical circulation changes during 1974–78. *J. Atmos. Sci.*, **39,** 1153–1162.

Mureau, R., J. D. Opsteegh and J. S. Winston, 1987: Simulation of the effects of tropical heat sources on the atmospheric circulation. *Mon. Wea. Rev.*, **115,** 856–870.

Nigam, S., I. M. Held and S. W. Lyons, 1986: Linear simulation of the stationary eddies in a general circulation model, Part I: The no-mountain model. *J. Atmos. Sci.*, **43,** 2944–2961.

Opsteegh, J. D., 1982: On the importance of the Hadley circulation for cross equatorial propagation of stationary Rossby waves. *Collected papers KNMI Workshop, On the theory and application of simple climate models to the problem of long range weather prediction.* R. Mureau, C. J. Kok and R. J. Haarsma, Eds., Meteorologisch Institute De Bilt, Koninklijk, Netherlands, 129 pp.

——, and H. M. van den Dool, 1980: Seasonal differences in the stationary response of a linearized PE-Model: Prospects for long range weather forecasting? *J. Atmos. Sci.*, **37,** 2169–2185.

Quiroz, R. S., 1983: The climate of the El Niño winter of 1982–83.—A season of extraordinary climate anomalies. *Mon. Wea. Rev.*, **111,** 1685–1706.

Ramanathan, V., 1987: The role of earth radiation budget studies in climate and general circulation research. *J. Geophys. Res.*, **92,** 4075–4095.

Rosen, R. D., and D. A. Salstein, 1985: Effect of initialization on diagnoses of NMC large scale circulation statistics. *Mon. Wea. Rev.*, **113,** 1321–1337.

Sardeshmukh, P. D., and I. M. Held, 1984: The vorticity balance in the tropical atmosphere of a GCM. *J. Atmos. Sci.*, **41,** 768–778.

——, and B. J. Hoskins, 1985: Vorticity balances in the tropics during 1982–83 El Niño–Southern Oscillation event. *Quart. J. R. Meteor. Soc.*, **111,** 261–278.

Schneider, E. K., and I. G. Watterson, 1984: Stationary Rossby wave propagation through easterly layers. *J. Atmos. Sci.*, **41,** 2069–2083.

Shukla, J., and M. Fennessy, 1988: Prediction of time mean atmospheric circulation and rainfall: Influence of Pacific SST anomaly. *J. Atmos. Sci.*, **45,** 9–28.

Simmons, A. J., 1982: The forcing of stationary wave pattern by tropical diabatic heating. *Quart. J. Roy. Meteor. Soc.*, **108,** 503–534.

Van den Dool, H. M., 1983: A possible explanation of the observed persistence of monthly mean circulation anomalies. *Mon. Wea. Rev.*, **111,** 539–544.

van Loon, H., and R. A. Madden, 1981: The Southern Oscillation. Part I: Global associations with pressure and temperature in northern winter. *Mon. Wea. Rev.*, **109,** 1150–1162.

Walker, G. T., 1923: Correlation in seasonal variations of weather, VIII. A preliminary study of world weather. Vol. 24, Part 4, Superintendent of Government Printing, Calcutta, 75–131.

Webster, P. J., 1972: Response of the tropical atmosphere to local steady forcing. *Mon. Wea. Rev.*, **100,** 518–541.

——, 1973: Temporal variations of the low latitude zonal circulations. *Mon. Wea. Rev.*, **101,** 803–816.

——, 1981: Mechanisms determining the atmospheric response to sea surface temperature anomalies. *J. Atmos. Sci.*, **38,** 554–571.

Yanai, M., S. Esbensen and J.-H. Chu, 1973: Determination of bulk properties of tropical cloud clusters from large scale heat and moisture budgets. *J. Atmos. Sci.*, **30,** 611–627.